THE JOURNAL OF BIOLOGICAL CHEMISTRY VOL. 284, NO. 31, pp. 21036–21046, July 31, 2009

Occludin Phosphorylation and Ubiquitination Regulate Tight Junction Trafficking and Vascular Endothelial Growth Factor-induced Permeability*[S]

Received for publication, January 20, 2009, and in revised form, May 4, 2009 Published, JBC Papers in Press, May 28, 2009, DOI 10.1074/jbc.M109.016766

Tomoaki Murakami, Edward A. Felinski, and David A. Antonetti[1]

From the Department of Cellular and Molecular Physiology and Ophthalmology, Penn State College of Medicine, Hershey, Pennsylvania 17033

Vascular endothelial growth factor (VEGF) alters tight junctions (TJs) and promotes vascular permeability in many retinal and brain diseases. However, the molecular mechanisms of barrier regulation are poorly understood. Here we demonstrate that occludin phosphorylation and ubiquitination regulate VEGF-induced TJ protein trafficking and concomitant vascular permeability. VEGF treatment induced TJ fragmentation and occludin trafficking from the cell border to early and late endosomes, concomitant with increased occludin phosphorylation on Ser-490 and ubiquitination. Furthermore, both co-immunoprecipitation and immunocytochemistry demonstrated that VEGF treatment increased the interaction between occludin and modulators of intracellular trafficking that contain the ubiquitin interacting motif, including Epsin-1, epidermal growth factor receptor pathway substrate 15 (Eps15), and hepatocyte growth factor-regulated tyrosine kinase substrate (Hrs). Inhibiting occludin phosphorylation by mutating Ser-490 to Ala suppressed VEGF-induced ubiquitination, inhibited trafficking of TJ proteins, and prevented the increase in endothelial permeability. In addition, an occludin-ubiquitin chimera disrupted TJs and increased permeability without VEGF. These data demonstrate a novel mechanism of VEGF-induced occludin phosphorylation and ubiquitination that contributes to TJ trafficking and subsequent vascular permeability.

Under normal physiological conditions the blood-brain barrier and blood-retinal barrier regulate the transport of water, ions, amino acids, and waste products, between the neural parenchyma and blood (1). A high degree of well developed tight junctions (TJs)[2] in the vascular endothelium, in association with adherens junctions, contribute to both the blood-brain and blood-retinal barriers (2). Accumulating evidence suggests that a number of pathological eye diseases such as diabetes, retinopathy of prematurity, age-related macular degeneration, inflammation, and infectious diseases disrupt the TJs altering the blood-retinal barrier. Common mediators of vascular permeability and TJ deregulation are growth factors and cytokines that may induce macular edema and lead to loss of vision (1). Vascular endothelial growth factor (VEGF), in particular, induces vascular permeability and stimulates angiogenesis, contributing to disease pathogenesis in diabetic retinopathy and retinopathy of prematurity (3). VEGF also contributes to blood-brain barrier disruption with subsequent edema and angiogenesis in brain tumors and stroke (4). Recent advances in biomedical research have provided therapeutic approaches to neutralize VEGF; however, these strategies have not yet demonstrated effective resolution of diabetic macular edema (5, 6).

TJs control the paracellular flux of solutes and fluids across the blood-brain and blood-retinal barriers. Several transmembrane proteins including occludin, tricellulin, the claudin family, and junction adhesion molecules are thought to confer adhesion to the TJ barrier and to be organized by members of the zonula occludens family (ZO-1, -2, or -3) (7–9). Experimental evidence has established that the claudins confer barrier properties and claudin-5 specifically contributes to the vascular component of the blood-brain barrier demonstrated by gene deletion studies (10). In contrast, the function of occludin in paracellular flux has remained less clear. Mice with occludin gene deletion continue to form TJs in gut epithelia with normal barrier properties (11). However, studies have also demonstrated that diabetes reduces occludin content in rat retina (12) and alters its distribution from continuous cell border localization to intracellular puncta (13). These observations suggest that the intracellular trafficking of TJ proteins promotes paracellular flux and vascular permeability in diabetic animals (12, 14).

VEGF was originally identified as a vascular permeability factor as well as a pro-angiogenic growth factor (15, 16). Both biological effects exacerbate the pathology of retinal vascular diseases (17), and they are mediated via intracellular signal transduction, especially based on the phosphorylation of Src, protein kinase C, and so on (18). Additionally, VEGF treatment and diabetes induce occludin phosphorylation in rat retinal vasculature and endothelial cell culture coincident with increased permeability (19). Recently, using mass spectrometry five occludin phosphorylation sites were identified in retinal endothelial cell culture after VEGF treatment (20). Among these sites, phosphorylation at Ser-490 was shown to increase in

* This work was supported, in whole or in part, by National Institutes of Health Grants EY 016413 and EY 012021 (to D. A. A.). This work was also supported by the Juvenile Diabetes Research Foundation International (to D. A. A.).

[S] The on-line version of this article (available at http://www.jbc.org) contains supplemental Figs. S1–S3.

[1] To whom correspondence should be addressed. Tel.: 717-531-5032; Fax: 717-531-7667; E-mail: dantonetti@psu.edu.

[2] The abbreviations used are: TJ, tight junction; VEGF, vascular endothelial growth factor; ZO-1, zonula occludens-1; UIM, ubiquitin interacting motif; Eps15, epidermal growth factor receptor pathway substrate 15; Hrs, hepatocyte growth factor-regulated tyrosine kinase substrate; BREC, bovine retinal endothelial cell; HA, hemagglutinin; WtOcc, V5-tagged wild-type occludin; S490AOcc, occludin mutants in which Ser-490 was substituted to alanine; Occ-Ub, occludin-ubiquitin chimeric protein; S490A-Ub, S490AOcc-ubiquitin chimeric protein; EV, empty vector; E3, ubiquitin-protein isopeptide ligase.

response to VEGF treatment. However, no evidence has directly demonstrated the contribution of occludin phosphorylation to VEGF-induced endothelial permeability or defined the mechanism by which phosphorylation of occludin alters paracellular flux.

Modification of proteins with monomeric or polymeric ubiquitin chains contributes to control of multiple biological functions including protein degradation, intracellular trafficking, translational regulation, and DNA repair (21). Phosphorylation of receptor tyrosine kinases, such as epidermal growth factor receptor or vascular endothelial growth factor receptor-2, is followed by ubiquitination and regulated trafficking to endosomes. This endocytosis process depends on the interaction between the ubiquitinated receptors and carrier proteins that possess a ubiquitin interacting motif (UIM) such as Epsin, epidermal growth factor receptor pathway substrate 15 (Eps15), and hepatocyte growth factor-regulated tyrosine kinase substrate (Hrs) (21–24). Recent publications have demonstrated that occludin can be ubiquitinated targeting the protein for degradation through the ubiquitin-proteasome system in epithelial cell types (25, 26). Here we demonstrate that phosphorylation of occludin at Ser-490 is necessary for occludin ubiquitination in response to VEGF in endothelial cells. Furthermore, the ubiquitination promotes interaction of occludin with UIM containing modulators of trafficking and regulates the internalization of TJ proteins altering endothelial permeability. Together, these results suggest that occludin phosphorylation and subsequent ubiquitination are necessary for VEGF-induced TJ trafficking and endothelial permeability.

EXPERIMENTAL PROCEDURES

Materials—Recombinant human $VEGF_{165}$ was purchased from R&D Systems (Minneapolis, MN). Complete protease inhibitor mixture tablets from Roche (Indianapolis, IN) were used. All other chemical reagents were obtained from Calbiochem or Sigma.

Occludin Expression Constructs and Mutants—Ser-490 of human occludin was substituted to alanine using the QuikChange Site-directed Mutagenesis Kit (Stratagene, La Jolla, CA) according to the manufacturer's instructions. Briefly, the mutation was introduced using the PCR primers, 5′-CTGAAGCAAGTGAAGGGAGCCGCAGATTACAAAAGTAAGAA-3′ and 5′-TTCTTACTTTTGTAATCTGCGGCTCCCTTCACTTGCTTCAG-3′, followed by digestion of the template using DpnI and transformation into competent cells. The wild-type and mutant occludin constructs in plasmid pENTR221 (Invitrogen) were subcloned into pUB6/V5-His expression vector (Invitrogen) using HindIII and XhoI sites. The full-length occludin sequences tagged with V5 and His were further sublconed to pmaxCloning™ expression vector (Amaxa Biosystems, Gaithersburg, MD) using HindIII and NheI sites.

Hemagglutinin (HA)-tagged ubiquitin in pMT123 was a kind gift of Dr. Vincent Chau. For the occludin-ubiquitin chimera construct, the ubiquitin sequence was amplified by PCR (forward primer; 5′-TACCGGTGCAAACATGCAGATCTTTGTGA-3′, reverse primer; 5′-GTTGTATTTCTGGGCTAGCTG-3′), which was subcloned into AgeI and NheI sites of pmaxCloning™ expression vector containing occludin mutants. Additionally, mutation for the stop codon after the ubiquitin sequence was introduced by the QuikChange Site-directed Mutagenesis Kit (Stratagene), using the substitution primers, 5′-GCGCCTGCGAGGTGGCTAAATTGAGCCTTCTCTCC-3′ and 5′-GGAGAGAAGGCTCAATTTAGCCACCTCGCAGGCGC-3′. All constructs were confirmed by sequencing.

Cell Culture—Primary bovine retinal endothelial cells (BRECs) were isolated and cultured as described previously (27, 28). Briefly, bovine retinas were homogenized and applied to the filtration steps to isolate the endothelial cells. BRECs were cultured in MCDB-131 medium (Sigma) supplemented with 10% fetal bovine serum (Hyclone, Logan, UT), 10 ng/ml epidermal growth factor (Sigma), 0.2 mg/ml endothelial cell growth medium additive (EndoGro; Vec Technologies, Rensselaer, NY), 0.09 mg/ml heparin (Fisher Scientific), and 0.01 mg/ml antibiotic-antimycotic (Invitrogen). When BREC reached confluence, medium was replaced with MCDB-131 supplemented with 1% fetal bovine serum, 0.01 mg/ml antibiotic-antimycotic, and 100 nM hydrocortisone, followed by further incubation for 24 h.

Immunocytochemistry—Localization of TJ proteins were evaluated by immunocytochemistry as described previously (29). Briefly, cells were plated on 12-mm diameter coverslips (Nunc, Naperville, IL) at a density of 1.5×10^5 cells/well. BRECs were fixed in 1% paraformaldehyde for 10 min, and permeabilized with 0.2% Triton X-100. After blocking with 10% goat serum, cells were incubated for 2 days with primary antibodies against occludin, claudin-5, ZO-1 (Zymed Laboratories Inc., South San Francisco, CA), early endosome antigen 1, clathrin heavy chain (Abcam, Cambridge, MA), lysosome-associated membrane protein 1 (BD Biosciences, San Diego, CA), Eps15 (Santa Cruz biotechnology, Santa Cruz, CA), Hrs (Alexis Biochemicals, San Diego, CA), and V5 (Invitrogen). Primary antibodies were detected with Alexa 488 anti-mouse, Alexa 555 anti-rabbit, and Alexa 647 anti-rat antibodies (Invitrogen) for 1 h. Single *en face* confocal sections were obtained using a confocal microscope (TCS SP2 AOBS; Leica, Wetzlar, Germany).

Colocalization of occludin and endosomal markers was evaluated using ImageJ Plugin. Briefly, after three areas were at random selected in each sample, colocalization of red and green signals was individually quantified and the ratio of colocalized/total occludin was averaged.

TJ integrity was quantified by scoring according to the grade of continuity. The area contained in each transfected cell was divided into a 7.2×7.2-μm grid. The continuity of immunoreactivity of TJ proteins in each grid was defined as: grade 1, less than 25% continuous border staining between cells; grade 2, ~25% continuous border staining; grade 3, ~50% continuous border staining; grade 4, most of the border is continuous with intermittent breaks; grade 5, all border staining is completely continuous. Twenty cells transfected with each occludin construct were selected at random, followed by masked grading. Frequency of the grading was calculated using all grids from all 20 cells. The significant difference between groups was determined by chi-square test.

Immunoblot Analysis—Western blot using the NuPAGE system (Invitrogen) was performed as described previously (29). After blocking with milk in Tris-buffered saline with 0.1% Tween 20, immunoblotting was performed using anti-claudin-5 (Zymed Laboratories Inc.), anti-Eps15, anti-Epsin-1 (Santa Cruz Biotechnology), anti-Hrs (Alexis Biochemicals), anti-ubiquitin (Biomol), anti-Itch (BD Biosciences), and anti-V5 (Invitrogen) antibodies. Mouse anti-occludin antibody (Zymed Laboratories Inc., number 33-1500) was used unless otherwise indicated. Antibody against phosphorylated occludin at Ser-490 was established as described previously (20). Primary antibodies were detected by horseradish peroxidase-conjugated anti-rabbit or anti-mouse IgG and chemiluminescence with ECL Plus (GE Healthcare).

Transfection—Transfection of plasmid containing occludin mutants or HA-tagged ubiquitin was achieved using the nucleofection technique (Amaxa Biosystems), according to the manufacturer's instructions (28). Briefly, after trypsinization of subconfluent BRECs, 5×10^5 cells per reaction were resuspended in 100 μl of HCAEC nucleofection solution (Amaxa Biosystems) supplemented with 3 μg of each plasmid, and applied by electroporation (setting S-005; Amaxa Biosystems). Transfected cells were grown in growth medium for 24 h, which was replaced by MCDB-131 with 1% fetal bovine serum. After serum starvation for an additional 24 h, BRECs were applied to each experiment.

Co-immunoprecipitation—The protein interactions were examined using co-immunoprecipitation of cell lysates, according to a modified protocol described previously (26). Briefly, BREC on 2 × 100-mm culture plates were lysed and homogenized with co-immunoprecipitation buffer (1% Nonidet P-40, 10% glycerol, 50 mM Tris, pH 7.5, 150 mM NaCl, 2 mM EDTA, 2 mM *N*-ethylmaleimide, 1 mM $NaVO_4$, 10 mM sodium fluoride, 10 mM sodium

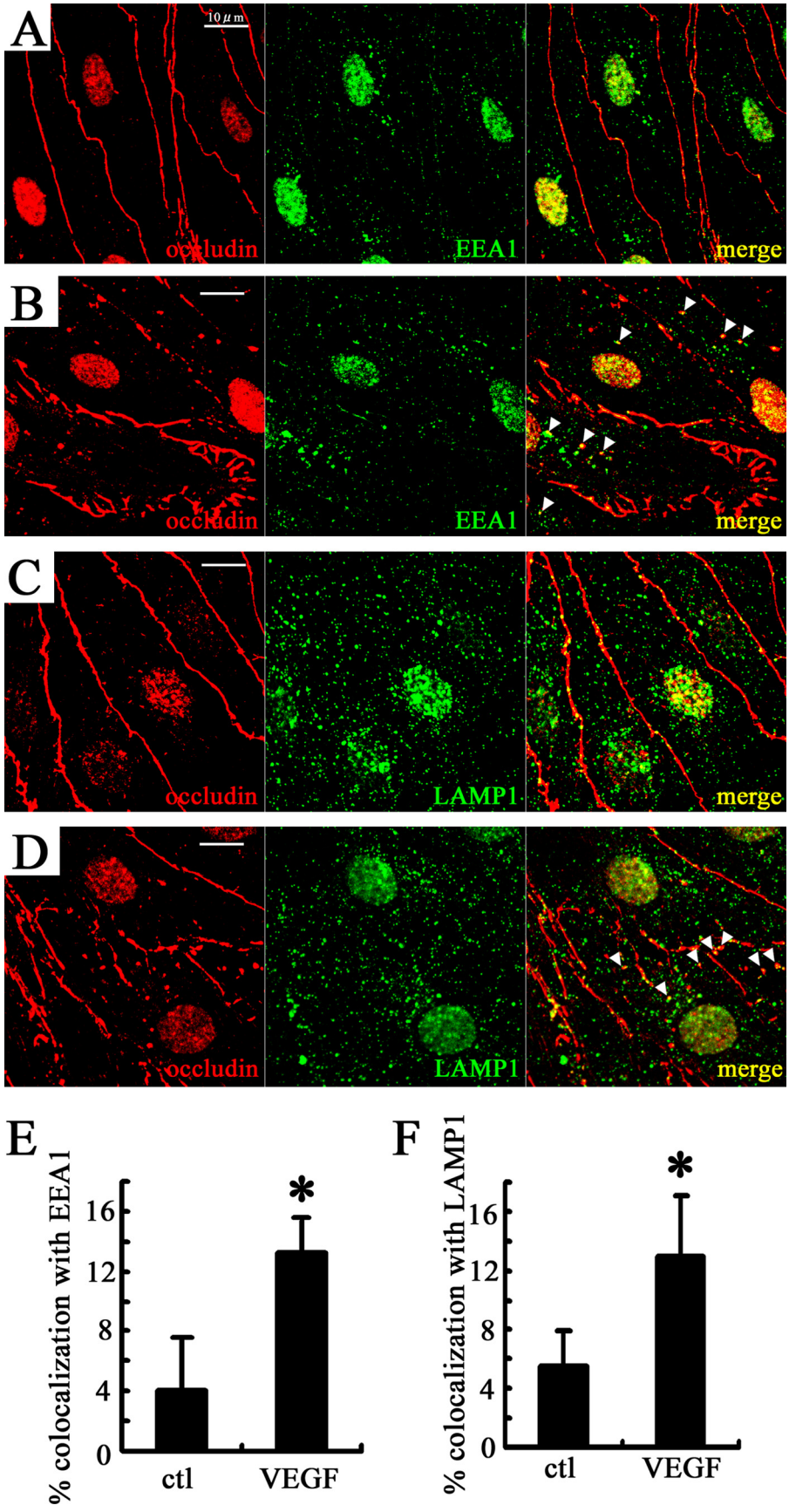

pyrophosphate, 1 mM benzamidine, complete protease inhibitor mixture). The lysate was centrifuged at 14,000 × *g* for 10 min, and the supernatant was transferred to another microcentrifuge tube. After a preclear with 100 μl of 1:1 slurry of Protein G-Sepharose™ 4 Fast Flow (GE Healthcare) for 1 h, the supernatant was incubated with each antibody for 2 h. Protein G beads were added, followed by further incubation for 1 h. The beads were recovered by centrifugation at 1500 × *g* for 1 min and washed four times with 1 ml of lysis buffer. Proteins bound to Protein G were eluted by boiling in Laemmli buffer for 5 min then used to Western blot, as described above.

Detection of Ubiquitination—BREC lysate was prepared using IP buffer (1% Nonidet P-40, 0.25% sodium deoxycholate, 0.1% SDS, 150 mM NaCl, 50 mM Tris, pH 7.5, 2 mM *N*-ethylmaleimide, 1 mM $NaVO_4$, 10 mM sodium fluoride, 10 mM sodium pyrophosphate, 1 mM benzamidine, complete protease inhibitor mixture). After the centrifugation, the supernatant was precleared with Protein G beads. Antibody against total occludin or phosphorylated occludin at Ser-490 or V5 for exogenous occludin was added and incubated for 2 h at 4 °C, followed by additional incubation with Protein G for 1 h. The beads were washed four times with lysis buffer, and boiled in Laemmli buffer. Eluted proteins were used for immunoblotting with anti-ubiquitin antibody.

HA-tagged ubiquitin was overexpressed and immunoprecipitated with anti-HA antibody (Roche). Immunoblotting with antibodies against occludin or phosphorylated occludin at Ser-490 was performed to evaluate whether the pool of ubiquitinated proteins contain these proteins.

In Vitro Permeability Assay—BRECs were cultured on filters with 0.4-μm pores (Transwell; Corning Costar, Acton, MA), as described previously (28). After VEGF treatment, 10 μM rhodamine B isothiocyanate-dextran (70 kDa) was added to the apical chamber of inserts. Aliquots were removed from the basolateral chamber every 30 min for 4 h after the application of dextran to the apical chamber and quantified. The rate of diffusive flux (P_o) was calculated by the following formula (30),

$$P_o = [(F_A/\Delta t)V_A]/(F_L A) \quad \text{(Eq. 1)}$$

where P_o is in centimeters per second; F_A is basolateral fluorescence; F_L is apical fluorescence; Δt is change in time; A is the surface area of the filter (in square centimeters); and V_A is the volume of the basolateral chamber (in cubic centimeters). Transendothelial electrical resistances were measured using an EVOM with a STX2 Electrode (World Precision Instruments, Sarasota, FL), just after the dextran permeability experiment (29).

Statistical Analysis—All experiments were repeated three or more times. Unless otherwise noted, statistical analysis was performed as follows. A two-tailed *t* test (two conditions) or analysis of variance (three or more conditions) was performed using software for statistical analysis (InStat 3.05; GraphPad). $p < 0.05$ was considered significant.

RESULTS

VEGF Disrupts TJ and Increases Occludin Trafficking to Early or Late Endosomes—Diabetes alters occludin distribution in rat retinas from a continuous cell border localization to intracellular puncta (13). To evaluate these changes in distribution, immunocytochemistry for occludin and markers of early and late endosomes was performed in BRECs. In untreated cells, immunoreactivity for occludin was continuous at the cell borders (Fig. 1*A*), whereas VEGF treatment (50 ng/ml, 15 min) disrupted occludin immunoreactivity at the cell border and increased intracellular punctate labeling, which co-localized with early endosome antigen 1 (Fig. 1, *B* and *E*). The intracellular puncta also co-localized with lysosome-associated membrane protein 1, which is a marker of late endosomes and lysosomes (Fig. 1, *D* and *F*). These data suggest that VEGF treatment induces occludin to traffic from the cell border to early and late endosomes.

VEGF Induces Occludin Ubiquitination, Which Requires Phosphorylation at Ser-490—The changes in the distribution of TJ proteins prompted us to investigate the molecular mechanism of VEGF-induced TJ trafficking. Ubiquitination of transmembrane proteins may induce endocytosis as observed for the epidermal growth factor receptor (21), therefore we tested the hypothesis that VEGF induces occludin ubiquitination, which modulates TJ trafficking. BRECs were treated with VEGF for the indicated times and immunoprecipitated with an antibody to occludin followed by immunoblotting with an antibody to ubiquitin. There was little occludin ubiquitination in the basal condition, but VEGF treatment increased occludin ubiquitination at ~66 and ~74 kDa as well as polyubiquitination in a time-dependent manner (Fig. 2*A*).

Because Ser-490 phosphorylation of occludin was shown to regulate interaction with ZO-1 (20), we investigated whether this phosphorylation site is involved in occludin ubiquitination. Immunoprecipitation with an antibody specific for Ser-490-phosphorylated occludin was followed by immunoblotting for ubiquitin. VEGF increased both occludin phosphorylation at Ser-490 and ubiquitination of this phospho-form of occludin (Fig. 2*B*).

For the additional confirmation of occludin ubiquitination, HA-tagged ubiquitin was transfected into BRECs using nucleofection (Amaxa) followed by immunoprecipitation of the HA tag. Western blotting demonstrated that total and Ser-490-phosphorylated occludin were ubiquitinated after VEGF treatment (Fig. 2*C*).

To elucidate the relationship between phosphorylation and ubiquitination, V5-tagged wild-type occludin (WtOcc) and occludin mutants in which Ser-490 was substituted to alanine

FIGURE 1. **VEGF disrupts continuous cell border staining of occludin, and increases the co-localization between occludin and endosomal markers in BREC.** *A* and *B*, double staining of occludin and early endosome antigen 1 (*EEA1*) in control (*A*) and after 15 min with 50 ng/ml VEGF treatment (*B*). *C* and *D*, immunolocalization of occludin and lysosome-associated membrane protein 1 (*LAMP1*) under control conditions (*C*) or after VEGF treatment (50 ng/ml, 15 min) (*D*). *Arrowheads*, puncta with co-localization. Background nuclear staining was also observed with secondary antibody alone (not shown). *Scale bar* = 10 μm. The co-localization was quantified (*E* and *F*). $n = 5$. *Error bars* represent the S.D. *, $p < 0.01$ *versus* control (*ctl*).

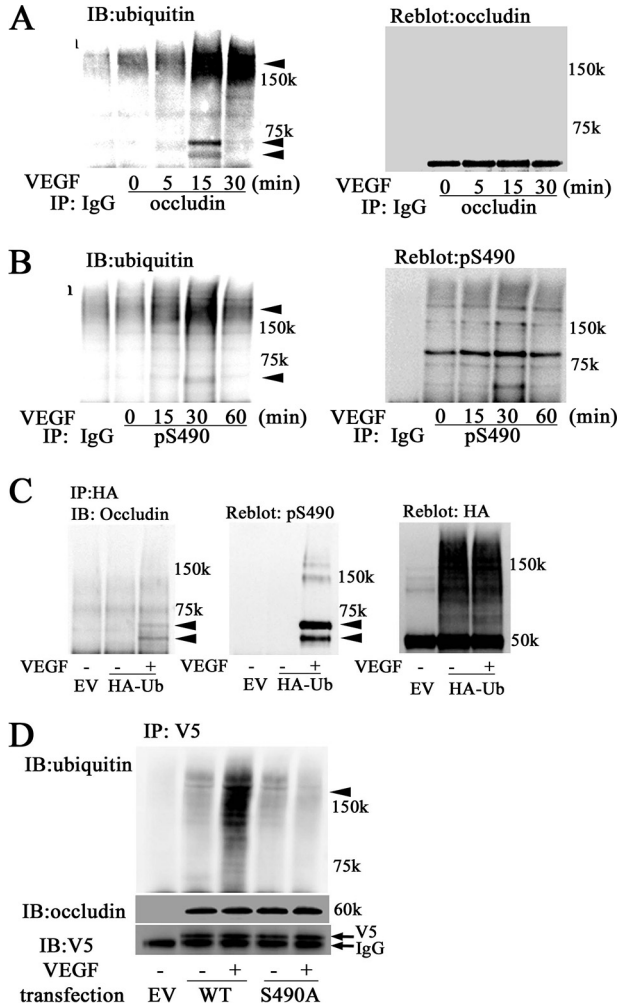

FIGURE 2. **VEGF increases occludin ubiquitination, dependent on phosphorylation at Ser-490.** *A*, BRECs treated with VEGF (50 ng/ml) over the time course indicated were used to detect the ubiquitination of occludin (*A*) and phospho-Ser-490 (*B*). *Arrowheads*, ubiquitinated occludin. *C*, occludin detected by rabbit occludin antibody (Zymed Laboratories Inc., 71–1500) and phospho-Ser-490 were also conjugated by exogenous ubiquitin after VEGF treatment (50 ng/ml for 15 min). *D*, VEGF treatment (50 ng/ml, 20 min) increased the ubiquitination of transfected WtOcc but not S490AOcc. *HA-Ub*, HA-tagged ubiquitin; *WT*, WtOcc; *S490A*, S490AOcc. *IB*, immunoblot; *IP*, immunoprecipitated.

(S490AOcc), were overexpressed in BRECs by nucleofection. Ubiquitination was determined by immunoprecipitation with anti-V5 antibody followed by Western blotting. WtOcc was ubiquitinated by VEGF treatment, whereas VEGF did not induce the ubiquitination of S490AOcc (Fig. 2*D*). These data demonstrate that phosphorylation at Ser-490 is necessary for VEGF-induced occludin ubiquitination.

VEGF Increases the Interaction between Occludin and the E3 Ligase Itch—Previous studies in epithelial cell types have demonstrated that the amine cytoplasmic domain of occludin interacts with the E3 ubiquitin ligase, Itch, leading to occludin ubiquitination (25, 26). We evaluated the interaction between occludin and Itch in response to VEGF treatment in BREC. Co-immunoprecipitation studies demonstrated that VEGF increased the interaction of Itch bound with occludin in a time-dependent manner, whether using either anti-occludin (Fig. 3*A*) or anti-Itch as the precipitating antibody (Fig. 3*B*). These

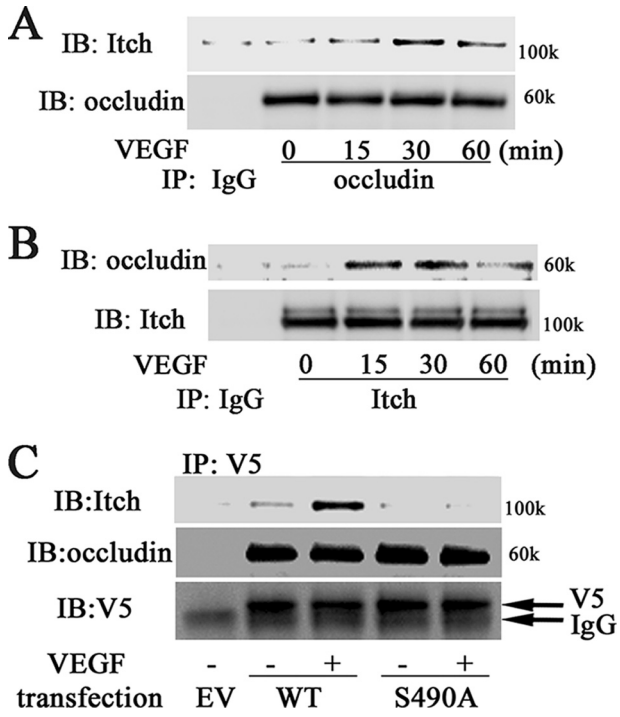

FIGURE 3. **VEGF induces the interaction between occludin and the E3 ligase, Itch, that requires occludin phosphorylation at Ser-490.** *A* and *B*, BRECs were incubated with VEGF (50 ng/ml) for the indicated time points, and used for co-immunoprecipitation (*IP*) studies with anti-occludin (*A*) or anti-Itch (*B*) antibody. The interaction between occludin and Itch was increased in a time-dependent manner. *C*, after transfection, WtOcc or S490AOcc were co-immunoprecipitated. VEGF (50 ng/ml, 15 min) increased the interaction between WtOcc and Itch, which was inhibited by S490AOcc. *WT*, WtOcc; *S490A*, S490AOcc. *IB*, immunoblot.

data demonstrate that VEGF induces an interaction between Itch and occludin.

Because occludin ubiquitination requires phosphorylation at Ser-490, the contribution of Ser-490 phosphorylation on occludin-Itch interaction was evaluated using WtOcc and S490AOcc. The V5-tagged wild-type and mutant occludin were transfected for co-immunoprecipitation studies. VEGF increased Itch interaction with WtOcc but Itch failed to coprecipitate with S490AOcc either with or without VEGF treatment (Fig. 3*C*). These data suggest that Itch-occludin interaction, as well as occludin ubiquitination, depends on the phosphorylation of occludin at Ser-490.

VEGF Promotes Occludin Endocytosis and Trafficking, Which Were Mediated via Epsin-1 and Eps15—Ubiquitinated transmembrane proteins are internalized by Epsin and Eps15 (31). These proteins recruit ubiquitinated transmembrane proteins to clathrin-coated pits or vesicles through UIM-ubiquitin binding, which promotes clathrin-mediated endocytosis of ubiquitinated proteins (21). Co-immunoprecipitation studies were performed to obtain biochemical evidence of occludin interaction with Epsin-1 and Eps15. Epsin-1 and Eps15 were both co-immunoprecipitated with anti-occludin antibody after VEGF treatment (Fig. 4*A*). Furthermore, VEGF increased the content of total occludin and phospho-Ser-490 occludin that was co-immunoprecipitated with anti-Epsin-1 or anti-Eps15 antibodies.

The interaction between occludin, Eps15, and clathrin was further evaluated by immunocytochemistry and confocal

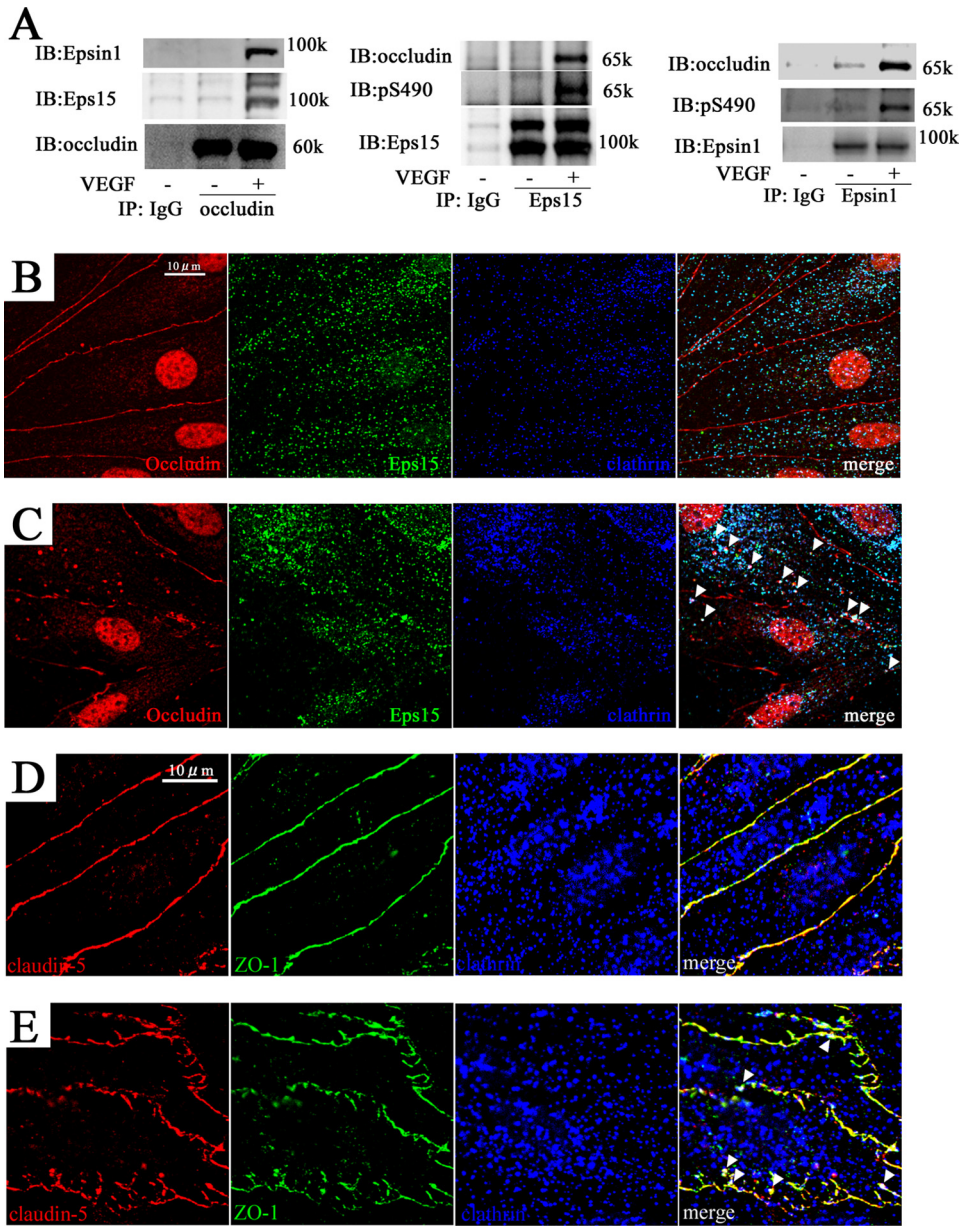

FIGURE 4. **VEGF promotes the interaction between occludin and Epsin-1 or Eps15.** *A*, co-immunoprecipitation (*IP*) with antibodies against occludin, Eps15, or Epsin-1 was performed in the absence or presence of VEGF (50 ng/ml, 15 min). VEGF increased the protein-protein interaction between total occludin (or phospho-Ser-490) and Eps15 or Epsin-1. Occludin was detected by rabbit occludin antibody (Zymed Laboratories Inc., 71-1500). *pS490*, phospho-Ser-490. Immunocytochemistry in the absence (*B* and *D*) or presence (*C* and *E*) of VEGF (50 ng/ml, 15 min) was performed. Compared with baseline, both TJ disruption and co-localization with clathrin (*arrowheads*) were observed after VEGF treatment. *Arrowheads*, co-localization of cytoplasmic puncta. *Scale bar* = 10 μm. *IB*, immunoblot.

microscopy. At baseline, occludin immunoreactivity was restricted to the cell border and both Eps15 and clathrin were distributed in the cytoplasm as puncta (Fig. 4*B*). In cells treated with VEGF, occludin immunoreactivity was discontinuous at the cell border with a concomitant increase in intracellular occludin puncta that co-localized with both Eps15 and clathrin immunoreactivity (Fig. 4*C*). The trafficking of claudin-5 and ZO-1 was also evaluated by immunocytochemistry. Similar to occludin, VEGF treatment disrupted cell border staining of these TJ proteins and increased the co-localization between clathrin and claudin-5 and ZO-1 (Fig. 4, *D* and *E*). Together these studies suggest that VEGF increases the ubiquitination of occludin, which leads to the interaction with Epsin-1 and Eps15 through UIM-ubiquitin binding and subsequent endocytosis. Furthermore, claudin-5 and ZO-1 also undergo clathrin-mediated endocytosis after VEGF treatment.

Interaction between Occludin and Hrs—Hrs contributes to the endosomal trafficking of ubiquitinated proteins through binding with the UIM (24, 32). The interaction between Hrs and ubiquitinated occludin after VEGF treatment was determined by immunocytochemistry and co-immunoprecipitation. In untreated cells, occludin immunoreactivity was continuous at the cell border, whereas Hrs was located in the cytoplasm. After VEGF treatment, occludin immunoreactivity co-localized to Hrs in puncta (Fig. 5*A*). Co-immunoprecipitation with anti-Hrs or anti-occludin antibody demonstrated that both total occludin and occludin phosphorylated at Ser-490 interact with Hrs in response to VEGF (Fig. 5*B*).

Contribution of Occludin Ser-490 Phosphorylation to TJ Endocytosis—Co-immunoprecipitation studies demonstrated VEGF-dependent interaction between Ser-490-phosphorylated occludin and endocytosis trafficking proteins, Epsin-1, Eps15, and Hrs (Figs. 4*A* and 5*B*). Furthermore, the S490AOcc mutant failed to undergo ubiquitination after VEGF treatment. These data led us to investigate whether Ser-490 phosphorylation is necessary for occludin endocytosis and TJ disruption. To determine whether phosphorylation at Ser-490 is required for the interaction with the UIM-containing proteins, co-immunoprecipitation studies with anti-V5 precipitating antibody were carried out after transfection of V5-tagged WtOcc and S490AOcc. Immunoblotting demonstrated that Epsin-1, Eps15, and Hrs co-immunoprecipitated with WtOcc after VEGF treatment. However, these same proteins failed to co-immunoprecipitate with S490AOcc regardless of VEGF treatment (Fig. 6*A*). These data suggest that VEGF-induced phosphorylation at Ser-490 is necessary for ubiquitination and the subsequent interaction between occludin and these UIM-containing proteins.

To further investigate whether VEGF-induced TJ disruption requires phosphorylated occludin at Ser-490, immunocyto-

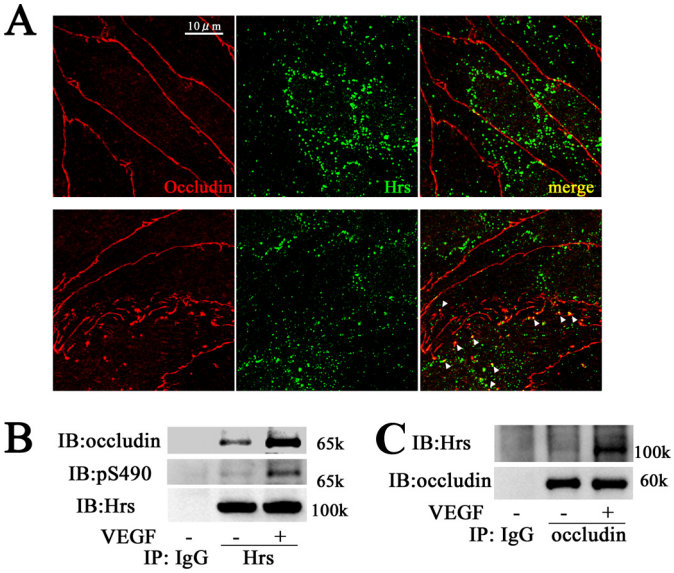

FIGURE 5. **VEGF promotes the interaction between occludin and Hrs.** Immunocytochemistry was performed on BREC without (*A*) or with (*B*) VEGF treatment (50 ng/ml, 15 min). At baseline, occludin did not colocalize with Hrs, whereas VEGF increased the intracellular punctate staining of occludin, which co-localized with Hrs (*arrowheads*). *C*, co-immunoprecipitation (*IP*) with anti-occludin or anti-Hrs antibody showed that the interaction was increased by VEGF. Occludin around 65 kDa was detected by rabbit occludin antibody (Zymed Laboratories Inc., 71-1500). *pS490*, phospho-Ser-490. *Scale bar* = 10 μm. *IB*, immunoblot.

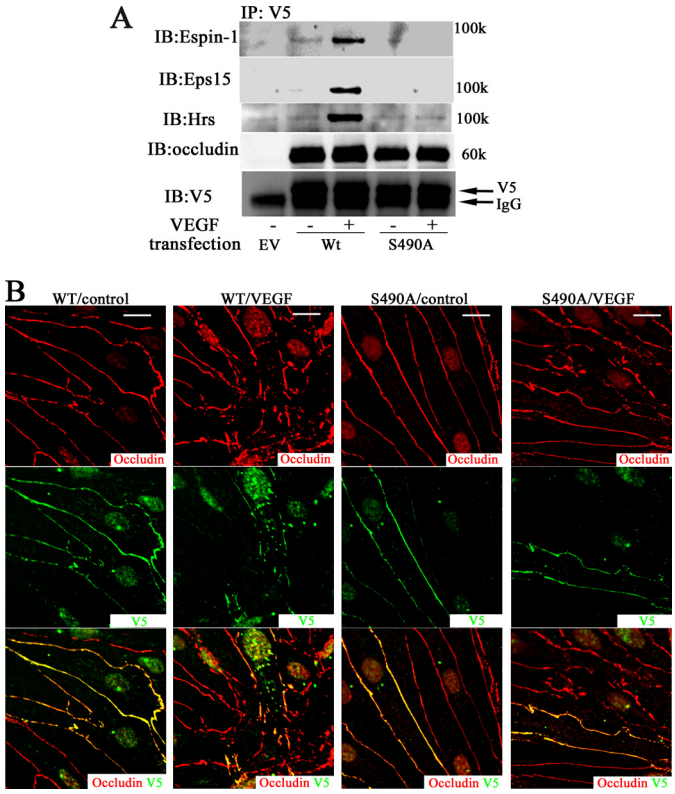

FIGURE 6. **S490AOcc mutant inhibits occludin trafficking.** *A*, WtOcc or S490AOcc was expressed and co-immunoprecipitated (*IP*) with V5 antibody. VEGF (50 ng/ml, 15 min) induced the interaction between WtOcc and Epsin-1, Eps15, or Hrs, whereas S490AOcc completely inhibited these interactions. *B*, immunocytochemistry demonstrated that VEGF disrupted continuous occludin staining in WtOcc-transfected cells, whereas transfection of the S490AOcc mutant prevented the VEGF-induced TJ disruption. These changes were quantified and presented in supplemental Fig. S3. *WT*, WtOcc; *S490A*, S490AOcc. *Scale bar* = 10 μm.

chemistry of the V5-tagged constructs was performed. Immunoreactivity for occludin, claudin-5, and ZO-1 was continuous at the cell border in WtOcc-transfected cells and disrupted by VEGF treatment (Fig. 6*B*, supplemental Fig. S1 and quantified in supplemental Fig. S3). However, BREC transfected with S490AOcc demonstrated continuous cell border immunolabeling for occludin, claudin-5, and ZO-1 and the addition of VEGF had no effect on the cellular distribution of these proteins. These data suggest that occludin phosphorylation at Ser-490 is required for occludin endocytosis and TJ disruption in response to VEGF treatment.

Occludin-ubiquitin Chimera Is Sufficient to Increase TJ Disruption without VEGF—To determine whether occludin ubiquitination is sufficient for the trafficking or disruption of TJ proteins, an occludin-ubiquitin chimeric protein was created by linking ubiquitin to the carboxyl tail of either WtOcc (Occ-Ub) or the S490AOcc mutant (S490A-Ub) and the constructs were tagged with V5 epitope at the carboxyl terminus. Co-immunoprecipitation of the Occ-Ub chimeras with anti-V5 antibody was performed after transfection of chimeras to evaluate the interaction with UIM-containing proteins. In the absence of VEGF, Epsin-1, Eps15, and Hrs were co-immunoprecipitated with Occ-Ub, whereas WtOcc had little co-precipitation of these proteins without VEGF treatment, despite higher expression relative to the chimeric proteins (Fig. 7*A*). Importantly, the S490A-Ub chimera also co-precipitated with the UIM-containing proteins, suggesting that the presence of the ubiquitin was sufficient to allow interaction with these trafficking proteins.

Immunocytochemistry was performed after the exogenous expression of the chimeric proteins. Compared with the appearance in WtOcc-transfected BRECs, immunolabeling of V5-tagged Occ-Ub presented large intracellular puncta. Furthermore, ZO-1 and claudin-5 immunolabeling at the cell border was disrupted, with increased intracellular punctate immunoreactivity for occludin (Fig. 7*B*, supplemental Figs. S2 and S3). The immunoreactivity for occludin, claudin-5, ZO-1, and V5 in S490A-Ub-transfected BRECs were similar to that in Occ-Ub-transfected cells. These data demonstrate that ubiquitination of occludin is sufficient to induce occludin endocytosis and disruption of the TJ complex with altered claudin-5 and ZO-1 border immunolabeling.

VEGF Induces Occludin Degradation by the Ubiquitin-proteasome Pathway—Previous studies demonstrated that VEGF decreased occludin content (12); therefore, the contribution of the ubiquitin-proteasome pathway was investigated. Occludin degradation rates were evaluated in the presence of cycloheximide (10 μg/ml), an inhibitor of protein biosynthesis, followed by Western blotting. Thirty min after MG132 (50 μM) treatment, cells were treated with VEGF and cycloheximide, then lysed at the indicated time. VEGF accelerated the rate of occludin degradation compared with control conditions ($p < 0.05$ in both time points, analysis of variance). Treatment with the proteasome inhibitor, MG132, prevented the increased rate of occludin degradation after VEGF treatment ($p < 0.01$ in both time points, analysis of variance) suggesting that proteasome inhibition completely prevented the VEGF-induced occludin

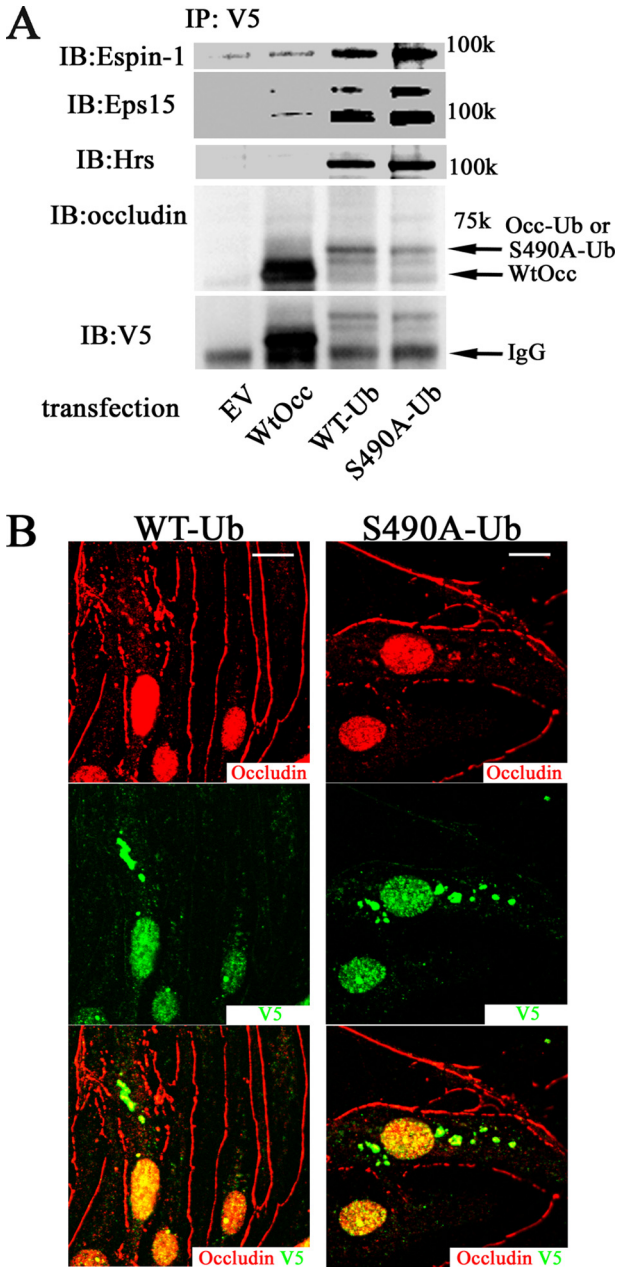

FIGURE 7. **Occludin-ubiquitin chimera induces occludin trafficking.** *A*, co-immunoprecipitation (*IP*) demonstrated that both Occ-Ub and S490A-Ub interact with Epsin-1, Eps15, and Hrs in the absence of VEGF. *B*, BRECs were transfected with these chimeric mutants for immunocytochemistry. Both Occ-Ub and S490A-Ub presented intracellular puncta, and cell border staining of occludin was fragmented in Occ-Ub- or S490A-Ub-transfected cells. *WT*, WtOcc. *Scale bar* = 10 μm. *IB*, immunoblot.

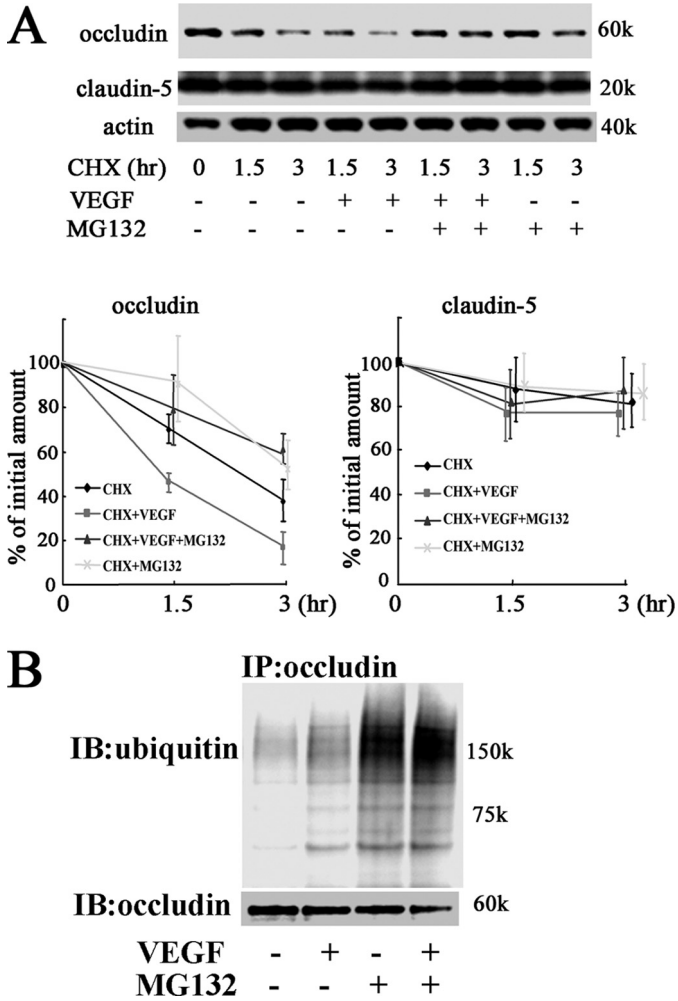

FIGURE 8. **VEGF-induced occludin degradation is mediated via the ubiquitin/proteasomal system.** *A*, after protein synthesis was inhibited by cycloheximide (*CHX*) (10 μg/ml) occludin content was evaluated by Western blotting. VEGF (50 ng/ml) enhanced the rate of occludin degradation, which was blocked by MG132 (50 μM). The rate of claudin-5 degradation was not changed by either VEGF or MG132. $n = 7–8$. *Error bars* represent the S.D. *B*, after the pretreatment with MG132 (50 μM), BRECs were treated with VEGF (50 ng/ml, 15 min). MG132 increased ubiquitinated occludin with or without VEGF. *IP*, immunoprecipitated; *IB*, immunoblot.

degradation (Fig. 8*A*). These data demonstrate that VEGF promotes occludin degradation, at least in part, through the ubiquitin-proteasome system. In contrast, there were no significant differences in the rate of claudin-5 degradation after VEGF treatment, suggesting that VEGF alters claudin-5 localization but does not induce claudin-5 degradation (Fig. 8*A*). Furthermore, MG132 increased mono- and polyubiquitinated occludin either with or without VEGF treatment (Fig. 8*B*). These data suggest that occludin is ubiquitinated under basal conditions and VEGF treatment increases occludin ubiquitination and proteasomal degradation. However, the degradation rate in this study was slow, compared with that observed in LLC-PK1 cells (25), and the reason for this difference in occludin ubiquitination and degradation in different cell types remains to be determined.

Phosphorylation and Ubiquitination of Occludin Regulates Vascular Permeability—The contribution of occludin phosphorylation and ubiquitination to endothelial permeability of 70-kDa-rhodamine B isothiocyanate dextran and transendothelial electrical resistance were evaluated in monolayers of BREC transfected with either WtOcc or S490AOcc. Compared with baseline, VEGF treatment increased the permeability of dextran in cells transfected with empty vector (EV) or WtOcc. However, transfection of S490AOcc completely blocked the permeability of dextran induced by VEGF treatment (Fig. 9*A*). In addition, VEGF decreased the electrical resistance and increased ion permeability in EV and WtOcc-transfected BREC. Transfection of S490AOcc blocked the VEGF-induced decrease in electrical resistance (Fig. 9*B*). These data demon-

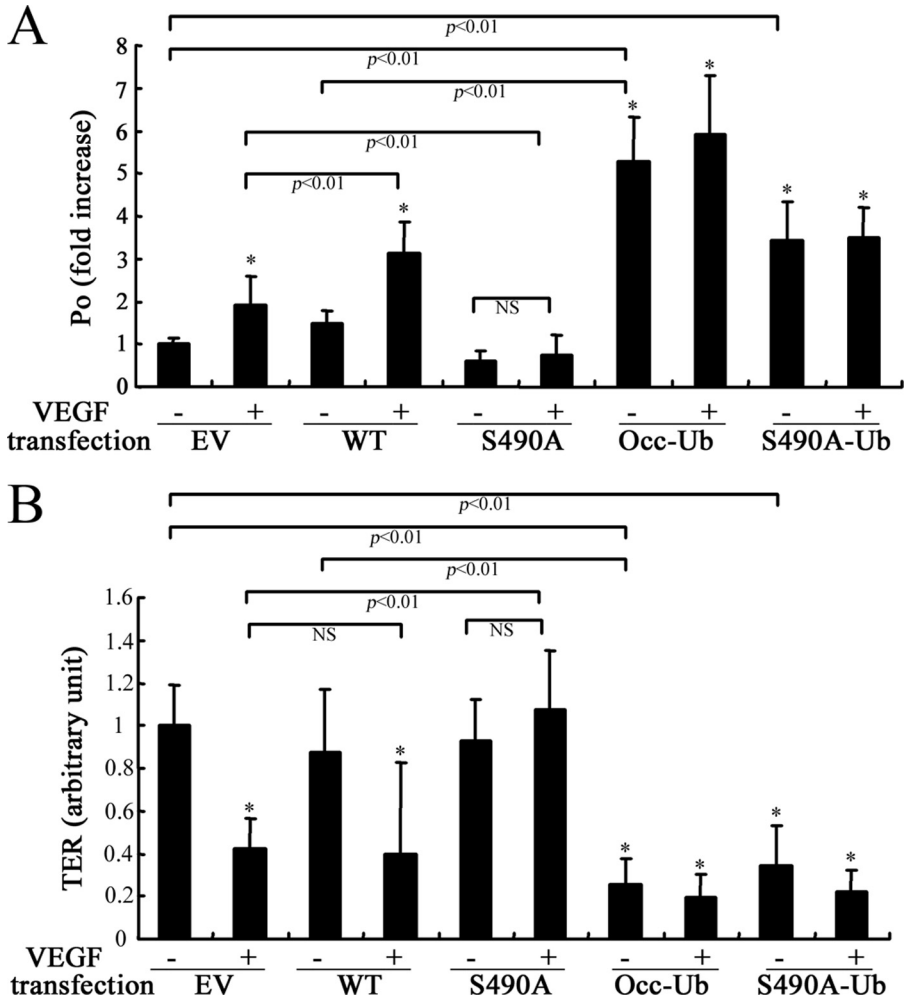

FIGURE 9. **Phosphorylation of occludin on Ser-490 and ubiquitination regulate VEGF-induced vascular endothelial permeability.** *A*, diffusive flux (P_o) of 70-kDa-dextran was evaluated in the absence or presence of VEGF (50 ng/ml), after the transfection of each occludin mutant. VEGF-induced hyperpermeability was inhibited by S490AOcc, whereas Occ-Ub and S490A-Ub increased the tracer flux without VEGF. *B*, transendothelial electrical resistance (*TER*) measurements. VEGF reduced the resistance, which was inhibited by S490AOcc. The chimera proteins decreased the resistance both with and without VEGF. $n = 7$–9. *Error bars* represent the S.D. * $p < 0.01$ *versus* EV-transfected cells without VEGF treatment. *WT*, WtOcc; *S490A*, S490AOcc. *NS*, not significant.

strate that phosphorylation of occludin at Ser-490 is necessary for VEGF-induced permeability in vascular endothelial cells with TJs.

Transfection of the Occ-Ub chimera increased the 70-kDa-dextran flux compared with EV control, and was not further increased with VEGF treatment (Fig. 9*A*). Transfection of the S490A-Ub chimera gave a similar result although not as pronounced, with increased permeability that was not further affected by VEGF. Measures of transendothelial electrical resistance demonstrated that the Occ-Ub chimera also increased ion permeability reducing electrical resistance and VEGF had no further effect. Again, the S490A-Ub chimera gave similar results (Fig. 9*B*). These data demonstrate that ubiquitination of occludin is sufficient for the disruption of TJ integrity and increased paracellular permeability in endothelial cells.

DISCUSSION

VEGF potently induces vascular permeability in most organ systems including the retina (16, 33). Both paracellular and transcellular routes of flux have been demonstrated as mechanisms of VEGF-induced permeability (2, 34). Although phenomenological changes in the junctional complex have been characterized suggesting increased paracellular transport, a detailed molecular mechanism of TJ regulation in response to VEGF has only begun to be elucidated. Recent publications have demonstrated that the internalization and trafficking of junctional proteins contribute to the increase in paracellular flux in several cell lines (35–37). In vascular endothelial cells, the adherens junction protein VE-cadherin is phosphorylated and internalized, which promotes VEGF-induced permeability (38). Here, we demonstrate a novel mechanism in which phosphorylation-dependent ubiquitination of occludin regulates VEGF-induced TJ disruption and vascular permeability in retinal vascular endothelial cells.

TJs are composed of both transmembrane adhesive proteins and scaffolding proteins and a number of regulatory proteins also localize to TJs (2, 9). The contribution to barrier properties has been clearly demonstrated for the transmembrane protein family, the claudins (10, 39), whereas the function of another transmembrane protein, occludin, has been ill-defined. Occludin was originally predicted to confer barrier properties to TJs (7, 40) and occludin gene deletion led to mice with an array of complex phenotypes but with normal TJ formation and barrier properties in gut epithelium (11, 41). However, there are many reports demonstrating that occludin contributes to or is altered in several pathological conditions (12, 42). These contradictory data led us to ask whether occludin confers barrier properties to paracellular flux *per se* or provides a regulatory function in the junctional complex. The results of our current study demonstrate a novel role for occludin in the regulation of paracellular permeability in endothelial cells with TJs, such as in the blood-brain barrier or blood-retinal barrier.

Evidence for both occludin phosphorylation and ubiquitin-mediated proteasomal degradation have previously been demonstrated (19, 25, 26, 43, 44). However, the mechanisms by which these modifications influence intracellular trafficking of TJ proteins, especially during VEGF-induced endothelial permeability, have not been elucidated. We now demonstrate that phosphorylation of occludin at Ser-490 in response to VEGF allows its ubiquitination, which leads to interaction with UIM

containing proteins, Epsin-1, Eps15, and Hrs, promoting clathrin-mediated endocytosis and trafficking to endosomes. Importantly, mutational analysis of occludin preventing phosphorylation at Ser-490 demonstrates that occludin phosphorylation and subsequent ubiquitination regulates the endocytosis of TJ proteins claudin-5 and ZO-1 in addition to occludin and controls endothelial permeability.

It is noteworthy that the intracellular puncta of occludin and claudin-5 (or ZO-1) appeared different after VEGF treatment compared with transfection of the occludin-ubiquitin chimera. This difference suggests that the chimeric protein is delayed in a specific trafficking compartment. Previous studies have demonstrated unique endocytosis pathways for TJ and adherens junction proteins (35) dependent on rab13 and rab8, respectively (45). The studies presented here demonstrate a coordination of occludin, claudin-5, and ZO-1 endocytosis to endosomes after VEGF treatment but the mechanisms that control targeting of occludin for degradation whereas claudin-5 is spared for potential recycling remains to be determined.

Recently, it was demonstrated that creating a phosphomimetic of Ser-490, S490D, does not affect the structure of the occludin coiled-coil domain but alters the charge distribution and reduces ZO-1 interaction (20, 46). In the current study, we demonstrate that phosphorylation at Ser-490 is necessary for VEGF-induced occludin ubiquitination. The critical steps for ubiquitination depend on the interaction between substrates and their E3 ligases. The first publication about the binding of occludin and its E3 ligase, Itch, showed that the amine terminus of occludin interacts directly with Itch (25). The amine terminus of occludin contains a PPYP sequence that interacts with the WW domain of Itch. Our data demonstrated the necessity of Ser-490 phosphorylation for Itch binding and occludin ubiquitination. It is unclear at this time how Ser-490 phosphorylation of occludin in the carboxyl terminus allows Itch binding in the amine terminus, but several possibilities may explain this phosphorylation-ubiquitination sequence. Phosphorylation at Ser-490 might decrease the interaction between occludin and other proteins, including ZO-1, exposing occludin to the E3 ligase. In addition, other phosphorylation sites on occludin or Itch may be essential for this process in conjunction with phosphorylation at Ser-490 (47). Alternatively, Ser-490 phosphorylation may increase the binding to ancillary proteins that promote Itch interaction and ubiquitination. The time course of occludin-Itch interaction is relatively longer compared with the ubiquitination and phosphorylation of occludin suggesting these additional molecular mechanisms should be considered along with the requirement of Ser-490 phosphorylation. Finally, deubiquitinating enzymes as well as occludin-Itch interaction may regulate the amount of ubiquitinated occludin.

In this study, both immunocytochemistry and biochemical analyses were used to demonstrate that VEGF increases occludin ubiquitination and endocytosis leading to ubiquitin-mediated proteasomal degradation. We speculate that the interaction between ubiquitinated occludin and Epsin-1 or Eps15 likely occurs via UIM, which subsequently promotes endocytosis (21). Likewise, occludin binds to the UIM containing protein Hrs, which also contributes to endosomal trafficking (24, 32). Recent publications have demonstrated a role of mono-, poly-, or multiple monoubiquitination in trafficking and interaction with Epsin-1 and Eps15 (31, 32, 48–50). Immunoprecipitation with Epsin-1 or Eps15 demonstrated a ~66-kDa occludin band that co-precipitated after VEGF treatment suggesting monoubiquitination of occludin because the molecular mass of occludin was originally reported to be ~58 kDa (40). Although we could not find evidence of polyubiquitinated occludin interacting with Epsin and Eps15, this possibility cannot be excluded because polyubiquitinated bands often present as a smear that may be difficult to detect in Western blotting. It remains to be determined whether mono-, poly-, or multiple monoubiquitination of occludin induces endocytic trafficking. Furthermore, the sequence of events that direct proteasomal degradation *versus* potential occludin recycling to the membrane has not yet been identified.

In our studies, overexpression of the OccS490A mutant dominated the endogenous occludin in regulation of TJ protein trafficking and endothelial permeability in response to VEGF. The precise mechanism by which the alanine mutation dominates remains to be determined but we speculate that the mutant interferes with the ability to recruit clathrin-mediated endocytosis-related proteins to TJs because the mutation prevents occludin ubiquitination. Furthermore, trafficking of TJs likely requires the contribution of additional TJ protein modifications or interactions with other modulators of endocytosis. Finally, transfection of Occ-Ub and S490A-Ub chimeras increased permeability without VEGF treatment suggesting that the occludin phosphorylation-ubiquitination sequence regulates TJ trafficking and that occludin ubiquitination is sufficient to confer barrier disruption and permeability. Ser-490 phosphorylation may also contribute to additional mechanisms regulating vascular permeability because the S490A-Ub chimera demonstrated less permeability than Occ-Ub in macromolecular tracer experiments.

Many studies have demonstrated a correlation of occludin content with permeability. Earlier studies of occludin overexpression in Madin-Darby canine kidney cells increased mannitol flux, whereas electrical resistance was also increased (51). Here we demonstrate that overexpression of WtOcc did not reduce permeability, but, in fact, significantly increased VEGF-induced permeability to 70-kDa dextran. These data support a model in which the amount of ubiquitinated occludin determines TJ disruption and vascular permeability rather than loss of occludin *per se*. Furthermore, this model suggests that occludin degradation acts as a negative feedback system for TJ integrity. Therefore, the content of occludin detected at the traditional 58 kDa correlates with barrier properties because occludin ubiquitination reduces the observed band at this molecular weight, induces TJ disruption, and over time leads to occludin degradation in endothelial cells. It is important to note that we failed to detect evidence of occludin ubiquitination in Madin-Darby canine kidney cells (data not shown) suggesting that occludin ubiquitination may be cell-type specific or limited to the VEGF response.

In conclusion, we demonstrate that VEGF induces phosphorylation-dependent occludin ubiquitination, which is necessary for increased permeability to both macromolecules and ions. These studies demonstrate a role for occludin in regulation of

endothelial barrier properties and suggest important potential therapeutic targets for the control of vascular permeability in diseases of the blood-brain and blood-retinal barrier.

REFERENCES

1. Antonetti, D. A., Barber, A. J., Bronson, S. K., Freeman, W. M., Gardner, T. W., Jefferson, L. S., Kester, M., Kimball, S. R., Krady, J. K., LaNoue, K. F., Norbury, C. C., Quinn, P. G., Sandirasegarane, L., and Simpson, I. A. (2006) *Diabetes* **55,** 2401–2411
2. Harhaj, N. S., and Antonetti, D. A. (2004) *Int. J. Biochem. Cell Biol.* **36,** 1206–1237
3. Aiello, L. P. (1997) *Invest. Ophthalmol. Vis. Sci.* **38,** 1647–1652
4. Machein, M. R., and Plate, K. H. (2000) *J. Neurooncol.* **50,** 109–120
5. Gardner, T. W., and Antonetti, D. A. (2008) *Curr. Diab. Rep.* **8,** 263–269
6. Dorrell, M., Uusitalo-Jarvinen, H., Aguilar, E., and Friedlander, M. (2007) *Surv. Ophthalmol.* **52,** Suppl. 1, S3–19
7. Hirase, T., Staddon, J. M., Saitou, M., Ando-Akatsuka, Y., Itoh, M., Furuse, M., Fujimoto, K., Tsukita, S., and Rubin, L. L. (1997) *J. Cell Sci.* **110,** 1603–1613
8. Morita, K., Sasaki, H., Furuse, M., and Tsukita, S. (1999) *J. Cell Biol.* **147,** 185–194
9. Matter, K., and Balda, M. S. (2003) *Nat. Rev. Mol. Cell Biol.* **4,** 225–236
10. Nitta, T., Hata, M., Gotoh, S., Seo, Y., Sasaki, H., Hashimoto, N., Furuse, M., and Tsukita, S. (2003) *J. Cell Biol.* **161,** 653–660
11. Saitou, M., Furuse, M., Sasaki, H., Schulzke, J. D., Fromm, M., Takano, H., Noda, T., and Tsukita, S. (2000) *Mol. Biol. Cell* **11,** 4131–4142
12. Antonetti, D. A., Barber, A. J., Khin, S., Lieth, E., Tarbell, J. M., and Gardner, T. W. (1998) *Diabetes* **47,** 1953–1959
13. Barber, A. J., Antonetti, D. A., and Gardner, T. W. (2000) *Invest. Ophthalmol. Vis. Sci.* **41,** 3561–3568
14. Barber, A. J., and Antonetti, D. A. (2003) *Invest. Ophthalmol. Vis. Sci.* **44,** 5410–5416
15. Leung, D. W., Cachianes, G., Kuang, W. J., Goeddel, D. V., and Ferrara, N. (1989) *Science* **246,** 1306–1309
16. Senger, D. R., Galli, S. J., Dvorak, A. M., Perruzzi, C. A., Harvey, V. S., and Dvorak, H. F. (1983) *Science* **219,** 983–985
17. Aiello, L. P., Avery, R. L., Arrigg, P. G., Keyt, B. A., Jampel, H. D., Shah, S. T., Pasquale, L. R., Thieme, H., Iwamoto, M. A., Park, J. E., Nguyen, M. D., Aiello, L. M., Ferrara, N., and King, G. L. (1994) *N. Engl. J. Med.* **331,** 1480–1487
18. Scheppke, L., Aguilar, E., Gariano, R. F., Jacobson, R., Hood, J., Doukas, J., Cao, J., Noronha, G., Yee, S., Weis, S., Martin, M. B., Soll, R., Cheresh, D. A., and Friedlander, M. (2008) *J. Clin. Invest.* **118,** 2337–2346
19. Antonetti, D. A., Barber, A. J., Hollinger, L. A., Wolpert, E. B., and Gardner, T. W. (1999) *J. Biol. Chem.* **274,** 23463–23467
20. Sundstrom, J. M., Tash, B. R., Murakami, T., Flanagan, J. M., Bewley, M. C., Stanley, B. A., Gonsar, K. B., and Antonetti, D. A. (2009) *J. Proteome Res.* **8,** 808–817
21. Di Fiore, P. P., Polo, S., and Hofmann, K. (2003) *Nat. Rev. Mol. Cell Biol.* **4,** 491–497
22. Duval, M., Bédard-Goulet, S., Delisle, C., and Gratton, J. P. (2003) *J. Biol. Chem.* **278,** 20091–20097
23. Huang, F., Kirkpatrick, D., Jiang, X., Gygi, S., and Sorkin, A. (2006) *Mol. Cell* **21,** 737–748
24. Raiborg, C., Bache, K. G., Gillooly, D. J., Madshus, I. H., Stang, E., and Stenmark, H. (2002) *Nat. Cell Biol.* **4,** 394–398
25. Traweger, A., Fang, D., Liu, Y. C., Stelzhammer, W., Krizbai, I. A., Fresser, F., Bauer, H. C., and Bauer, H. (2002) *J. Biol. Chem.* **277,** 10201–10208
26. Lui, W. Y., and Lee, W. M. (2005) *J. Cell. Physiol.* **203,** 564–572
27. Antonetti, D. A., and Wolpert, E. B. (2003) *Methods Mol. Med.* **89,** 365–374
28. Harhaj, N. S., Felinski, E. A., Wolpert, E. B., Sundstrom, J. M., Gardner, T. W., and Antonetti, D. A. (2006) *Invest. Ophthalmol. Vis. Sci.* **47,** 5106–5115
29. Phillips, B. E., Cancel, L., Tarbell, J. M., and Antonetti, D. A. (2008) *Invest. Ophthalmol. Vis. Sci.* **49,** 2568–2576
30. Chang, Y. S., Munn, L. L., Hillsley, M. V., Dull, R. O., Yuan, J., Lakshminarayanan, S., Gardner, T. W., Jain, R. K., and Tarbell, J. M. (2000) *Microvasc. Res.* **59,** 265–277
31. Polo, S., Sigismund, S., Faretta, M., Guidi, M., Capua, M. R., Bossi, G., Chen, H., De Camilli, P., and Di Fiore, P. P. (2002) *Nature* **416,** 451–455
32. Barriere, H., Nemes, C., Du, K., and Lukacs, G. L. (2007) *Mol. Biol. Cell* **18,** 3952–3965
33. Aiello, L. P., Bursell, S. E., Clermont, A., Duh, E., Ishii, H., Takagi, C., Mori, F., Ciulla, T. A., Ways, K., Jirousek, M., Smith, L. E., and King, G. L. (1997) *Diabetes* **46,** 1473–1480
34. Dvorak, A. M., Kohn, S., Morgan, E. S., Fox, P., Nagy, J. A., and Dvorak, H. F. (1996) *J. Leukocyte Biol.* **59,** 100–115
35. Ivanov, A. I., Nusrat, A., and Parkos, C. A. (2004) *Mol. Biol. Cell* **15,** 176–188
36. Matsuda, M., Kubo, A., Furuse, M., and Tsukita, S. (2004) *J. Cell Sci.* **117,** 1247–1257
37. Shen, L., and Turner, J. R. (2005) *Mol. Biol. Cell* **16,** 3919–3936
38. Gavard, J., and Gutkind, J. S. (2006) *Nat. Cell Biol.* **8,** 1223–1234
39. Furuse, M., and Tsukita, S. (2006) *Trends Cell Biol.* **16,** 181–188
40. Furuse, M., Hirase, T., Itoh, M., Nagafuchi, A., Yonemura, S., Tsukita, S., and Tsukita, S. (1993) *J. Cell Biol.* **123,** 1777–1788
41. Schulzke, J. D., Gitter, A. H., Mankertz, J., Spiegel, S., Seidler, U., Amasheh, S., Saitou, M., Tsukita, S., and Fromm, M. (2005) *Biochim. Biophys. Acta* **1669,** 34–42
42. Dallasta, L. M., Pisarov, L. A., Esplen, J. E., Werley, J. V., Moses, A. V., Nelson, J. A., and Achim, C. L. (1999) *Am. J. Pathol.* **155,** 1915–1927
43. Sakakibara, A., Furuse, M., Saitou, M., Ando-Akatsuka, Y., and Tsukita, S. (1997) *J. Cell Biol.* **137,** 1393–1401
44. Bojarski, C., Weiske, J., Schöneberg, T., Schröder, W., Mankertz, J., Schulzke, J. D., Florian, P., Fromm, M., Tauber, R., and Huber, O. (2004) *J. Cell Sci.* **117,** 2097–2107
45. Yamamura, R., Nishimura, N., Nakatsuji, H., Arase, S., and Sasaki, T. (2008) *Mol. Biol. Cell* **19,** 971–983
46. Li, Y., Fanning, A. S., Anderson, J. M., and Lavie, A. (2005) *J. Mol. Biol.* **352,** 151–164
47. Gao, M., Labuda, T., Xia, Y., Gallagher, E., Fang, D., Liu, Y. C., and Karin, M. (2004) *Science* **306,** 271–275
48. Duncan, L. M., Piper, S., Dodd, R. B., Saville, M. K., Sanderson, C. M., Luzio, J. P., and Lehner, P. J. (2006) *EMBO J.* **25,** 1635–1645
49. Barriere, H., Nemes, C., Lechardeur, D., Khan-Mohammad, M., Fruh, K., and Lukacs, G. L. (2006) *Traffic* **7,** 282–297
50. Woelk, T., Oldrini, B., Maspero, E., Confalonieri, S., Cavallaro, E., Di Fiore, P. P., and Polo, S. (2006) *Nat. Cell Biol.* **8,** 1246–1254
51. Balda, M. S., Whitney, J. A., Flores, C., González, S., Cereijido, M., and Matter, K. (1996) *J. Cell Biol.* **134,** 1031–1049